I&EC research
Industrial & Engineering Chemistry Research

pubs.acs.org/IECR
Article

Hydrogen Peroxide-Mediated Oxidation of Biobased Poly(thioether-ester) Nanoparticles in Aqueous Medium

Published as part of Industrial & Engineering Chemistry Research special issue "Celebrating the Legacy of Prof. Jose M. Asua: Emulsion Polymerization and Polymer Reaction Engineering".

Kainan A. Weege, Priscilla B. Cardoso, Tamara Agner, Claudia Sayer, Ana P. S. Immich, Michael A. R. Meier, and Pedro H. H. de Araújo*

Cite This: https://doi.org/10.1021/acs.iecr.6c00305

ABSTRACT: Biobased poly(thioether-ester) (PTEe) nanoparticles were synthesized via thiol−ene miniemulsion polymerization using a sustainable monomer, offering a biodegradable alternative to fossil-derived polymers. To address intrinsic limitations such as hydrophobicity and low thermal stability, postpolymerization oxidation with hydrogen peroxide was employed to convert thioether groups into sulfoxide and sulfone functionalities. Two oxidation strategies were evaluated: direct latex oxidation and solution-phase oxidation. Both approaches effectively increased polymer polarity and thermal stability while preserving nanoparticle morphology. Structural analysis by IR spectroscopy confirmed the formation of sulfoxide and sulfone groups, while ^{1}H NMR indicated complete thiol−ene conversion. Thermal analysis revealed a marked rise in melting temperature (from 71 °C to 138−148 °C), while contact angle measurements showed enhanced surface hydrophilicity (θ reduced from 104° to 77−80°). Notably, latex oxidation (L-OXI) significantly improved nanoparticle stability and resistance to enzymatic degradation by CalB. This enhanced resistance is attributed to the incorporation of sulfoxide/sulfone groups, which stiffen the polymer matrix and restrict enzyme access to ester bonds.

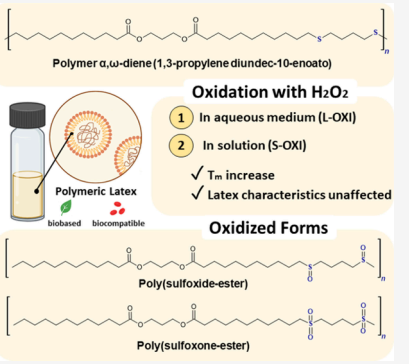

1. INTRODUCTION

Polymers derived from biobased monomers obtained from vegetable oils represent a promising sustainable alternative to fossil-based polymers, especially for medical applications when biocompatibility and/or biodegradability are required.[1−3] To meet the increasing demand for sustainable materials, significant efforts have been directed toward synthesizing polymers from renewable monomers with tunable functionalities.[4]

Polymers from fully renewable monomers bearing an ester, ether, or amide group at the polymer backbone have been successfully synthesized by thiol−ene polymerization.[5,6] Moreover, polymeric nanoparticles have been prepared via one-pot thiol−ene polymerization in miniemulsion.[7] The synthesis of poly(thioether-ester) nanoparticles via thiol−ene miniemulsion polymerization using plant-oil-derived monomers offers multiple environmentally friendly advantages, including the exclusive use of renewable feedstocks.[8] Previous studies have shown that thioethers can be oxidized to sulfoxides or sulfones or that they alter the properties of the polymer, including polarity, stiffness, and mechanical properties.[9−13]

Thiol−ene polymerizations can be considered as click or green chemistry reactions because they can be carried out under mild conditions, usually reach high conversion, and provide a high atom economy.[14,15] Also, miniemulsion polymerization uses water as a continuous medium avoiding the use of organic solvents, and it enables the production of polymeric nanoparticles with unique characteristics.[16−18]

Poly(thioether-ester) nanoparticles are particularly interesting for biomedical applications, as the ester group, which can undergo hydrolysis, potentially enables their degradation in a physiological environment.[19,20] However, flexible sulfide bonds in thioether linkages hinder the facile achievement of materials with a high glass transition temperature (T_g) when utilizing conventional thiol−ene combinations.[21,22] Furthermore, thioethers are typically regarded as hydrophobic compounds owing to their remarkably low dipole moment. Nevertheless, the hydrophobic nature of thioethers can be altered through oxidation, leading to the formation of sulfoxide and/or sulfone derivatives with increased dipole moments.[23−25] Consequently, the heightened polarity attributed to sulfone groups tends to augment the material's glass transition temperature and thermal

Received: January 20, 2026
Revised: April 22, 2026
Accepted: April 30, 2026
Published: May 18, 2026

stability.[22,23,26] Additionally, other polymer properties of thioethers, including flexural strength and optical transparency, change when they are oxidized to sulfoxides or sulfones.[26] Many organosulfur compounds and their derivatives exhibit different biological activities, and,[27] for example, the bactericidal activity can be enhanced by oxidation.[28] Also, thioether-containing macrocycles can act as protein−protein interaction inhibitors, and the protein interactions can be modulated by tuning the sulfur oxidation states with hydrogen peroxide (H_2O_2).[29,30]

The combination of both thioether and ester bonds within the polymer backbone could provide nanoparticles that are potentially sensitive to oxidation and hydrolysis, acting as dual-stimuli-responsive nanocarriers.[31] Among the different oxidants and catalysts for thioether oxidation, hydrogen peroxide stands out as the most versatile, commercially available, low-cost, and comparably low-toxic and environmentally friendly option.[27,32] When H_2O_2 is used as an oxidant, thioethers can be efficiently oxidized to sulfoxides and, with further slow oxidation, to sulfones.[11,32,33] Moreover, the oxidation of sulfides using hydrogen peroxide typically proceeds under relatively mild conditions, often requiring only a slight excess of H_2O_2,[24,32,34] with water being the only byproduct of the reaction.[27,32] Additionally, hydrogen peroxide is suitable for oxidizing poly(thioether) particles dispersed in aqueous media due to its solubility in water.[29,35]

In this study, the sulfur atoms in the backbone of poly(thioether-ester) nanoparticles were oxidized to sulfoxides and sulfones using a hydrogen peroxide solution. The structural characterization of the synthesized monomer and of the nonoxidized poly(thioether-ester) nanoparticles prepared via thiol−ene polymerization in miniemulsion was performed by proton nuclear magnetic resonance (^{1}H NMR) spectroscopy. The samples were also characterized using Raman spectroscopy and Fourier-transform infrared spectroscopy (FTIR). Thermogravimetric analysis (TGA) and differential scanning calorimetry (DSC) evaluated the effect of postpolymerization modification on the thermal properties of the polymers, while changes in nanoparticle size, morphology, and colloidal stability were assessed using dynamic light scattering (DLS) and transmission electron microscopy (TEM). Furthermore, the surface wettability of the materials was investigated through contact angle measurements, providing further information about the changes in surface properties caused by oxidation. The enzymatic degradation assays were performed on the original and on the oxidized nanoparticle colloidal dispersions, respectively, samples latex and L-OXI, using *Candida antarctica* lipase B (CalB) in a PBS solution, and the degradation products were characterized by FTIR, TGA, and DLS.

2. EXPERIMENTAL SECTION

2.1. Materials

10-Undecenoic acid (98%, Sigma-Aldrich), 1,3-propanediol (99.6%, Sigma-Aldrich), p-toluene sulfonic acid monohydrate (98.5%, Sigma-Aldrich), aluminum oxide (activated, basic, Brockmann I, Sigma-Aldrich), magnesium sulfate (anhydrous, ≥ 99.5%, Sigma-Aldrich), sodium dodecyl sulfate − SDS (99%, Sigma-Aldrich), 2,2′-azobis(2-methylpropionitrile) − AIBN (98%, Sigma-Aldrich), 1,4-butanedithiol (>97%, Sigma-Aldrich), hydrogen peroxide solution (35 wt %, Neon Comercial), and sodium bicarbonate (99.7%, Vetec) were all used as received. Toluene (≥99.5%, Dinâmica), hexane (98.5%, Synth), diethyl ether (98%, Êxodo Científica), methanol (≥99.8%, Synth), and chloroform (≥99.8%, Êxodo Científica) were used. *Candida antarctica* Lipase B (commercial name: Lipozyme CalB L) was kindly donated by Novozymes. Distilled water was used in all experiments.

2.2. Synthesis of the Biobased Monomer

The biobased monomer 1,3-propylene diundec-10-enoate was synthesized as previously described by Cardoso et al. (2018). Briefly, 10-Undecenoic acid (0.27 mol), 1,3-propanediol (0.11 mol), p-toluenesulfonic acid (0.0157 mol), and toluene (200 mL) were mixed under magnetic stirring and heated to reflux. During the reaction, the water formed was collected by using a Dean−Stark apparatus. After 3 h, the reaction was complete and the reaction mixture was cooled. The purification of the product included toluene removal under reduced pressure and filtration through a short pad of basic aluminum oxide using hexane as the eluent. Finally, the solution was dissolved in diethyl ether (200 mL) and washed twice with water (200 mL) and dried over anhydrous $MgSO_4$, and the diethyl ether was removed under reduced pressure. The monomer synthesized was analyzed by ^{1}H NMR spectroscopy.

2.3. Synthesis of Poly(thioether-ester) Nanoparticles by Thiol−Ene Miniemulsion Polymerization

Poly(thioether-ester) nanoparticles were synthesized by miniemulsion polymerization. The aqueous phase was prepared by dissolving the surfactant SDS (3.5 wt % in relation to the monomer mass) in water (9.8 g), and the organic phase was prepared by mixing 1,3-propylene diundec-10-enoate (1.0 g) with the organic-soluble initiator AIBN (1.5 mol % in relation to the monomer). Both phases were magnetically stirred until complete solubilization of the surfactant and initiator. The aqueous phase was added to the organic phase and magnetically stirred (10 min, 500 rpm) to form a coarse emulsion. Then, 1,4-butanedithiol (1:1 dithiol-to-diene molar ratio) was added to the coarse emulsion, and the mixture was stirred (250 rpm) for another 5 min. Finally, the emulsion was sonicated for 3 min using a Fisher Scientific Model 500 Sonic Dismembrator (70% amplitude, pulse cycle: 10 s on/10 s off, 70%, using an ice bath). The polymerization was carried out at 80 °C for 4 h without stirring. The polymer obtained was analyzed by FTIR, TGA, DSC, NMR, DLS, and contact angle measurements.

2.4. Oxidation of Poly(thioether-ester) Nanoparticles

The postpolymerization oxidation process was performed following the experimental procedure previously reported.[37] This oxidation was conducted through two distinct routes: a) directly in the polymeric latex (Figure 1(a)) and b) in solution, after isolation of the polymer by

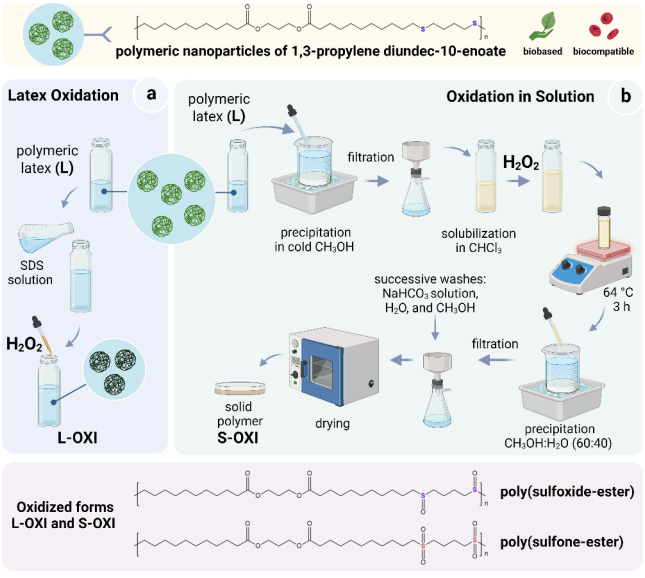

Figure 1. Postpolymerization oxidation process of poly(thioether-ester) nanoparticles carried out (a) directly in the polymeric latex and (b) in solution.

https://doi.org/10.1021/acs.iecr.6c00305
Ind. Eng. Chem. Res. XXXX, XXX, XXX−XXX

precipitation (Figure 1(b)). One aliquot of the poly(thioether-ester) latex (L) was directly oxidized in the aqueous medium (L-OXI). Therefore, 2 g of latex L (ca. 0.2 g of polymer) was mixed with 6 g of an SDS solution (0.25 wt %) in water, and then 0.6 mL of a hydrogen peroxide solution (35 wt %) was added dropwise. Another aliquot of the latex L was precipitated in cold methanol, and the polymer was oxidized in solution (S-OXI). In this case, 0.2 g of the precipitated polymer was dissolved in chloroform (20 mL), and then 0.6 mL of hydrogen peroxide solution (35 wt %) was added. After 3 h of reaction at 64 °C, the oxidized polymer was precipitated in a methanol−water mixture (60:40) and then successively washed with sodium bicarbonate (100 mL), water (100 mL), and methanol (100 mL) before being dried in a vacuum oven at room temperature.

2.5. Degradation of Poly(thioether-ester) Nanoparticles

Degradation assays of the polymeric nanoparticles (NPs) were conducted using a phosphate-buffered saline (PBS) system, as previously described.[38] The PBS buffer (0.2 M, pH 7.4) was prepared with distilled water, sodium chloride (NaCl), potassium chloride (KCl), anhydrous sodium phosphate monobasic (NaH_2PO_4, P.A. 99%, Vetec), and anhydrous sodium phosphate dibasic (Na_2HPO_4, P.A. 98%, Vetec). The enzymatic reaction was catalyzed by liquid form *Candida antarctica* lipase B (CalB).

The degradation conditions for both nonoxidized latex and oxidized (L-OXI) versions are summarized in Table 1. For the nonoxidized latex, 2.5 g of the latex from the miniemulsion polymerization was diluted in 7.5 g of a 0.25% SDS aqueous solution and added to 20 mL of a PBS solution (0.2 M, pH 7.4) containing 1 g of a free CalB enzyme aqueous solution (solid content of 23%). For the oxidized latex, 10 g of the oxidized latex was added to 20 mL of a PBS solution (0.2 M, pH 7.4) with 1 g of the free CalB enzyme in an aqueous solution. These amounts were calculated to equalize the polymer concentrations in both latexes, ensuring that the same mass of polymer was used in the degradation process. The enzymatic degradation was conducted under enzyme-excess conditions to ensure that the process was not limited by enzyme availability, allowing for a direct comparison of the intrinsic degradation behavior of the polymers. To determine the total solid content of the commercial CalB enzyme aqueous solution (Lipozyme CalB L), gravimetric analysis and TGA analyses of the dry CalB enzyme were performed.

Table 1. Formulations of Degradation Reactions

Component	Nonoxidized Latex (Initial)	Oxidized Latex (L-OXI)
Latex	2.5 g (227 mg of polymer)	10 g (227 mg of polymer)
SDS solution (0.25%)	7.5 g	—
PBS solution	20 g	20 g
CalB aq. solution[a]	1 g	1 g

[a]Solid content of 23% (w/w).

The reactions were carried out in a round-bottom flask under continuous agitation at 37 °C. Degradation kinetics were monitored over time intervals of 5, 10, 15, 30, 45, 60, 90, and 180 min to evaluate the enzymatic hydrolysis in PBS. The use of standardized CalB concentration in the assays aimed at ensuring consistent and comparable reaction conditions, enabling a direct evaluation of the effect of polymer oxidation on enzymatic degradation.

Degradation was evaluated on the basis of changes in particle size, the appearance of degradation products, and complementary analyses by TGA and FTIR.

2.6. Effect of pH on the Stability of Poly(thioether-ester) Nanoparticles

The stability of both nonoxidized (latex) and oxidized (L-OXI) poly(thioether-ester) nanoparticles under different pH conditions was evaluated by dynamic light scattering (DLS) and ζ-potential measurements. All analyses were conducted at the same solid content (23%) to ensure comparability between samples.

Aliquots of each nanoparticle dispersion (5 drops) were diluted in 20 mL of distilled water under gentle magnetic stirring (250 rpm) at room temperature. The initial pH of the diluted samples was measured (approximately 7.0). The pH was then adjusted to target values of 3.0, 5.0, 7.0, 9.0, and 11.0 using 0.1 M hydrochloric acid (HCl) for acidic pH and 0.1 M sodium hydroxide (NaOH) for basic pH. The pH was monitored with a calibrated pH meter, and the adjustment was performed dropwise under continuous stirring to avoid local overshooting. After pH adjustment, the samples were incubated at room temperature (25 °C) for 24 h without agitation. The hydrodynamic diameter (Z-average), polydispersity index (PdI), and zeta potential were measured immediately after pH adjustment (t = 0) and after 24 h of incubation (t = 24 h) using a Zetasizer Nano S instrument (Malvern Instruments, UK) at 25 °C. All measurements were performed in triplicate.

2.7. Determination of Enzymatic Activity

The enzymatic activity was determined based on the esterification reaction between lauric acid and propanol in a 1:1 molar ratio.[39] To homogenize the system, the mixture was kept under agitation at 250 rpm and 60 °C for 60 min. Prior to the addition of the enzyme, an aliquot was collected for blank titration. After this collection, 5% by mass of enzyme (relative to the substrates) was added. The esterification reaction proceeded for 60 min, after which a 150 μL aliquot was collected, diluted in 20 mL of an acetone:ethanol (1:1) solution, and subjected to titration with 0.04 N NaOH.

Enzymatic activity was defined as the amount of enzyme required to consume 1 μmol of lauric acid per minute. The calculation performed is described in eq 1

$$\frac{U}{g} = \frac{[(V^{0}NaOH) - (V^{60}NaOH)]\cdot N\cdot 10^{3}}{t\cdot ma} \quad (1)$$

where N is the molarity of the NaOH solution; $V^{0}NaOH$ and $V^{60}NaOH$ are the volumes of NaOH consumed (in mL) to titrate, respectively, the blank (sample at time zero) and the sample (sample at 60 min); t is the reaction time in min; and ma is the mass of the enzyme used in g.

2.8. Characterization

2.8.1. Structural and Chemical Characterization. The ^{1}H NMR spectra were recorded on a Bruker Ascend 600 spectrometer operating at 400 MHz. The samples were dissolved in deuterated chloroform ($CDCl_3$), and the spectra were acquired at 25 °C with 32 scans. Chemical shifts (δ) are reported in parts per million (ppm) relative to the residual solvent peak 7.26 ppm for $CDCl_3$ as an internal reference. The Attenuated Total Reflectance−Fourier Transform Infrared (ATR-FTIR) spectra of the polymer samples in KBr pellets were collected on a Shimadzu spectrometer, model IRPrestige-21, in the wavenumber range of 4000−400 cm^{-1} by accumulating 32 scans at a resolution of 4 cm^{-1}. Structural characterization and identification of functional groups of the samples were performed using Raman Spectroscopy. The analyses were carried out on a Cora 5001 Raman spectrometer (Anton Paar), equipped with excitation lasers at 532 and 785 nm. Spectra were collected in a wavenumber range from 1400 to 500 cm^{-1}.

2.8.2. Thermal Properties. Thermal decomposition was studied using thermogravimetric analysis − TGA (STA 449 F3 Jupiter, Netzsch). Approximately 10 mg of the polymeric samples was weighed in a platinum pan and heated from 25 to 600 °C, at a heating rate of 5 °C min^{-1}, under a nitrogen flow rate of 20 mL min^{-1}. The melting temperature (T_m) of NPs was determined by differential scanning calorimetry − DSC (Mettler Toledo DSC 823 calorimeter). The samples were heated from −50 to 210 °C at a heating rate of 10 °C min^{-1}. T_m was recorded from the second heating ramp.

2.8.3. Particle Properties and Surface Properties. Intensity average diameters of the polymer particles (Dp) and the dispersity (PDI) were measured by dynamic light scattering (DLS) using a Zetasizer Nano S from Malvern Instruments. Latex samples were diluted before measurement at 25 °C. The morphology of the nanoparticles was observed by Transmission Electron Microscopy using a JEM-1400 TEM (Jeol) electron microscope, operated at an

https://doi.org/10.1021/acs.iecr.6c00305
Ind. Eng. Chem. Res. XXXX, XXX, XXX−XXX

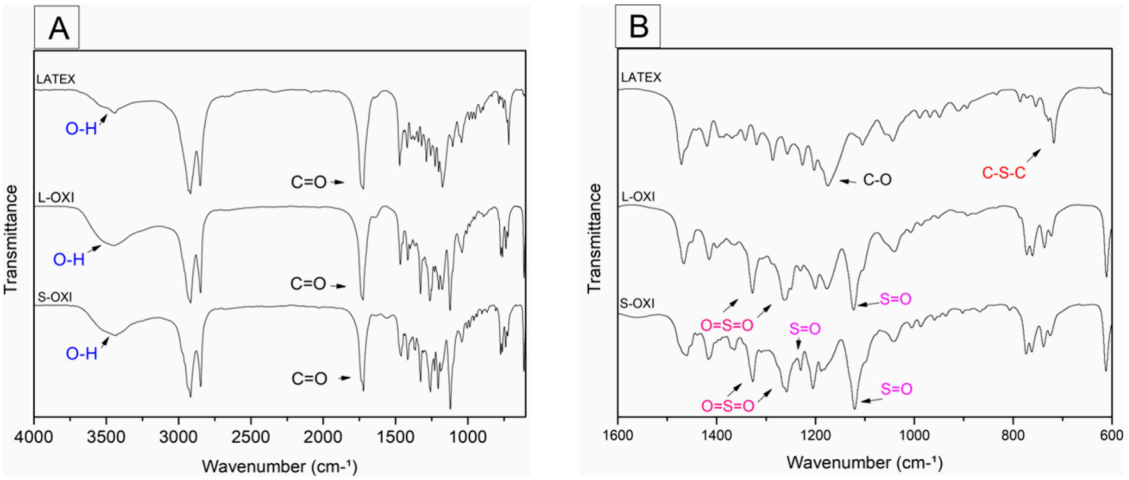

Figure 2. FTIR spectra of the Latex, L-OXI, and S-OXI. (A) full spectrum; (B) enlarged view from 1600 to 550 cm^{-1}.

accelerating voltage of 120 kV. A single droplet of the diluted latex (0.1% of solid content) was placed on a carbon-coated copper grid. The grid was dried overnight under room conditions. Different regions were analyzed to ensure that representative images were obtained. The static contact angle (θ) of the samples was measured using a goniometer (Ramé-hart Model 250). Polymer films were prepared by placing a known amount of each sample (Latex, L-OXI, and S-OXI) onto glass slides and heating them above their respective melting temperatures to allow film formation. After solidification at room temperature, the films were carefully detached from the slides, and the surface that had been in contact with the glass slide was used for contact angle measurements.

A droplet of ultrapure water (5 μL) was carefully deposited onto the polymer film using an automatic pipet. Measurements were performed at room temperature (25 °C), and at least three independent measurements were taken at different locations on the sample surface to ensure representative results.

2.8.4. Molecular Weight and Solubility. The molecular weight distribution and number and weight-average molecular weights (M_n, M_w) of the polymer samples were obtained by gel permeation chromatography (GPC) using high-performance liquid chromatography equipment (HPLC, model LC 20-A, Shimadzu) equipped with an SIL-20A auto sampler, a PL gelMiniMIX precolumn (5 μm, 50 × 4 mm) followed by two PL gel MiniMIX columns (5 μm, 250 × 4.6 mm) in series, and an RID-10A refractive index detector in THF as the eluent at a flow rate of 0.3 mL min^{-1}. The analyses were performed at 40 °C, and the samples (2.5 mg mL^{-1}) were filtered through a 0.22 μm PTFE membrane before injection. A calibration curve was constructed using polystyrene standards with molecular weight ranging from 580 to 9,225,106 g mol^{-1}, and data processing was carried out using the software LabSolutions and Origin. The dispersity (Đ) was calculated as the ratio M_w/M_n. The insoluble polymer content was determined using a polymer solution with a known concentration in tetrahydrofuran (THF), allowing it to dissolve for 48 h. Subsequently, the soluble phase was filtered using a glass syringe and a 0.45-μm nylon filter. The vials and filters were dried in a forced convection oven at 60 °C for 48 h. The insoluble polymer content was then calculated based on eqs 2 and 3, where the amount of retained polymer was first calculated (considering the polymer retained in the vial and filter (eq 2) and then the percentage of insoluble polymer was calculated (eq 3))

$$m_{PR} = (m_{VS} + m_{FS}) - (m_V - m_F) \quad (2)$$

$$P_R = \frac{m_{PR}}{m_P} \cdot 100 \quad (3)$$

where $m_{PR}m_{PR}$ is the mass of the polymer retained after evaporation of the volatiles; $m_{VS}m_{VS}$ and $m_{FS}m_{FS}$ are, respectively, the masses of the vial and of the filter after drying with the sample; m_Vm_V and m_Fm_F are the masses of the empty vial and of the filter; m_Pm_P is the mass of the polymer used to prepare the solution; and m_Rm_R is the percentage of insoluble polymer.

3. RESULTS AND DISCUSSION

To synthesize the diene monomer 1,3-propylene diundec-10-enoate, an esterification reaction was performed between 1,3-propanediol and 10-undecenoic acid. Poly(thioether-ester) (PTE) nanoparticles were obtained via thiol−ene miniemulsion polymerization using the diene monomer and butanedithiol (1,4 BDT). Then, the thioether-linkage moieties of the polymer chains within the nanoparticles obtained by thiol−ene miniemulsion polymerization were oxidized to sulfoxide and sulfone linkages using hydrogen peroxide.

The efficiency of the thiol−ene reaction is confirmed based on the NMR analysis by the consumption of the C═C double bonds as shown in the Supporting Information. The most important evidence, besides the ene consumption, is the emergence of new signals that confirm the formation of the thioether (C−S−C) bond. The ^{1}H NMR spectrum of the formed polymer shows a reduction in the relative intensities of the two peaks attributed to $CH{=}CH_2$, indicating the consumption of double bonds (5.85−5.76 ppm),[36] from the diene monomer during the thiol−ene polymerization reaction, suggesting the formation of PTEe.[39] New peaks at 2.58−2.44 ppm and 1.74−1.64 ppm were assigned to the polymer backbone (−CH− and $-CH_2-$), while the aliphatic chain signals (δ = 1.31−1.15 ppm) retained their relative integrals, indicating structural consistency. The ^{1}H NMR spectrum of 1,3-propylene diundec-10-enoate is consistent with literature data, confirming the expected structure and purity of the synthesized compound.[40]

Monomer

^{1}H NMR (400 MHz, $CDCl_3$, δ): 5.83−5.72 (m, 2H, 2 × $-CH{=}CH_2$), 5.01−4.89 (m, 4H, 2 × $-CH{=}CH_2$), 4.18 (t, 4H, J = 6.1 Hz, 2 × $-CH_2OCO-$), 2.33 (t, 4H, J = 7.3 Hz, CH_2COO-), 2.08 (m, 4H, 2 × $-CH_2-CH{=}CH_2$), 2.00−1.90 (m, 2H, J = 6.1 Hz, CH_2CH_2OCO-), 1.65−1.53 (m, 4H, 2 × CH_2CH_2COO-), 1.41−1.33 (m, 4H, 2 × CH_2) 1.31−1.15 (br.s, 16H, 2 × [4CH_2]) ppm.

Polymer

^{1}H NMR (400 MHz, $CDCl_3$, δ): 4.14 (t, J = 6.3 Hz, 4H, 2 × $-CH_2OCO-$), 2.60−2.41 (m, 8H, 4 × CH_2S), 2.29 (t, J = 7.3 Hz, 4H, 2 × CH_2CO-), 1.96 (p, J = 6.3 Hz, 2H), 1.76−1.65 (m, 4H,

https://doi.org/10.1021/acs.iecr.6c00305
Ind. Eng. Chem. Res. XXXX, XXX, XXX−XXX

2 × CH_2C), 1.63−1.49 (m, 10H, 5 × CH_2C), 1.42−1.09 (br.s, 24H, 2 × [12CH_2]) ppm.

FTIR spectra of the dried original latex and of the dried oxidized samples (L-OXI and S-OXI) are presented in Figure 2. FTIR analysis reveals distinct vibrational signatures corresponding to the oxidation of the polymers.

The ether bonds stretching (−C−O−) are assigned to the band at 1098 cm^{-1}, while the stretching of (−C−O−) and (−C═O) bonds of the ester groups are observed respectively at 1170 cm^{-1} and 1730 cm^{-1}. Additionally, the presence of a C−S−C stretching vibration can be observed at 720 cm^{-1}, indicating the addition of thiyl radicals across the double bonds of the diene during polymerization.[20] The oxidation of the polymer resulted in the appearance of two prominent new bands, the characteristic S═O stretching vibration at 1022−1030 cm^{-1} confirms sulfoxide (R_2S═O) formation, while the appearance of symmetric (1126 cm^{-1}) and asymmetric (1257 cm^{-1}) O═S═O stretching modes provides unambiguous evidence of sulfone (R−SO_2−R) groups, indicating progressive sulfur oxidation.[29,37,41] According to Infante Teixeira et al.[29] the kinetic analysis revealed that sulfones and sulfoxides coexisted during the process until complete conversion into polysulfones was observed, highlighting the importance of developing selective reaction control methods to obtain pure sulfoxide products. Certainly, the oxidation of thioether groups to sulfoxide and sulfone increases the material's polarity, which could promote water adsorption and explain the broad band at 3450 cm^{-1}.

The structural characterization and identification of the functional groups of the samples (latex, oxidized versions L-OXI, and S-OXI) were also performed using Raman spectroscopy and are shown in Figure 3.

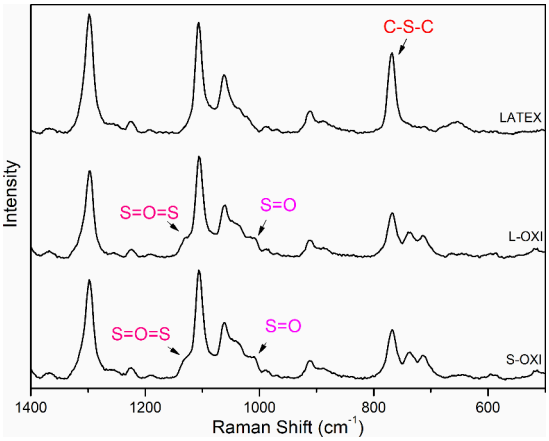

Figure 3. Raman spectra of the Latex and the oxidized samples L-OXI and S-OXI.

Raman spectroscopy is a critical analytical tool for validating the chemical transformation of the poly(thioether-ester) nanoparticles.[42] This technique identified the appearance of new vibrational modes associated with the highly polar sulfoxide and sulfone, which allowed for the clear distinction between the latex sample and the oxidized ones.

The oxidized versions (L-OXI and S-OXI) display new peaks at 738 cm^{-1} and 712 cm^{-1}. These peaks are often attributed to C−S stretching vibrations in the newly formed sulfoxide (R-S(O)-R') or, if the oxidation is extensive, the sulfone (R-$S(O)_2$-) structure. Specifically, the conversion of a single C−S−C band into a doublet or set of peaks suggests different conformations or local environments of the C−S bond in the oxidized product. The presence of characteristic peaks at 1124 cm^{-1} and 1025 cm^{-1} confirms the successful oxidation of the thioether groups in the synthesized polymers. The peak at 1124 cm^{-1} is attributed to the symmetric stretching vibration of the sulfone (SO_2) group, which forms when thioethers are fully oxidized by hydrogen peroxide (H_2O_2). Simultaneously, the peak at 1025 cm^{-1} corresponds to the sulfoxide (S═O) stretching vibration, indicating the presence of partially oxidized thioether units. These results, along with the previous ones, point out that the oxidation process in the aqueous dispersion was successful.

The thermal degradation of the polymers was evaluated by thermogravimetry, and the results are displayed in Figure 4A. The oxidation state of the sulfur atoms influences the thermal degradation of the polymers,[43] and the thermogravimetric analysis revealed distinct degradation profiles between the nonoxidized (latex) and oxidized (L-OXI, S-OXI) polymers.

All samples showed negligible mass loss below 100 °C, confirming the absence of volatile impurities or water.[44] The unmodified Latex sample exhibited a gradual mass loss starting at 220 °C (5%). In contrast, both oxidized variants (L-OXI and S-OXI) show no significant mass loss below 250 °C, confirming their enhanced stability in this temperature range due to the introduction of sulfur−oxygen bonds.

Notably, the nearly overlapping curves of L-OXI and S-OXI indicate that the oxidation method has enhanced the thermal stability, emphasizing that the oxidation state of sulfur governs the degradation behavior. The results align with DSC data (Figure 4B), where the nonoxidized Latex sample exhibited a melting temperature (T_m) of 71 °C with a ΔH_m of 4.99 J/g. After oxidation, both oxidized samples showed a substantial increase in T_m, reaching 138 °C for L-OXI and 148 °C for S-OXI, indicating that the introduction of polar sulfoxide and sulfone groups leads to the formation of thermally more stable crystalline domains. However, the ΔH_m values decreased to 1.94 J/g for L-OXI and 1.59 J/g for S-OXI, reflecting a reduction in the overall crystallinity degree. Using the nonoxidized Latex sample as a reference, the relative crystallinity of the oxidized samples was calculated to be 38.9% for L-OXI and 31.9% for S-OXI. The broader peaks of the oxidized samples are attributed to the recrystallization of the different crystalline forms in polar polymeric materials.[37] No clear Tg was observed between −50 and 0 °C for any of the samples. Both oxidation methods, solution (S-OXI) and latex (L-OXI), presented similar results.

Particle size distribution (PSD) of the poly(thioether-ester) nanoparticles before (L) and after oxidation (L-OXI), see Figure 5, shows that both the particle size and dispersity of the polymeric latex were not affected by the oxidation process. The particle size remained at about 130 nm with PdI values close to 0.1, indicating that the samples have a narrow size distribution, as shown in Table 2.

Hydrogen peroxide oxidizes nonpolar thioether moieties into more polar sulfoxide groups, altering the hydrophilic/hydrophobic balance.[45,46] Therefore, the contact angles of the oxidized versions were evaluated. All samples were washed to remove excess SDS and residual hydrogen peroxide. The decrease of the contact angle values of L-OXI and S-OXI in comparison to those of the latex reveals surface modifications caused by oxidation. The results are presented in Table 2.

However, the difference between the wetting of L-OXI and that of S-OXI was limited. The increased hydrophilicity of the oxidized derivatives was due to dipolar interactions between the

https://doi.org/10.1021/acs.iecr.6c00305
Ind. Eng. Chem. Res. XXXX, XXX, XXX−XXX

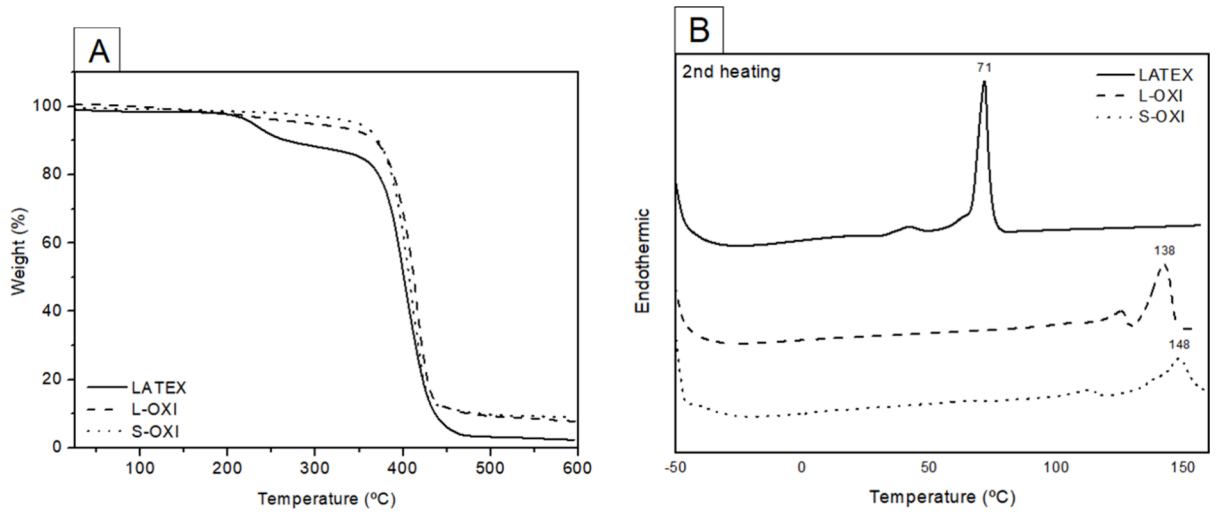

Figure 4. (A) TGA of the poly(thioether-ester) latex (**L**) and its oxidized forms (**L-OXI** and **S-OXI**). (B) DSC of latex (**L**) and its oxidized forms (**L-OXI** and **S-OXI**).

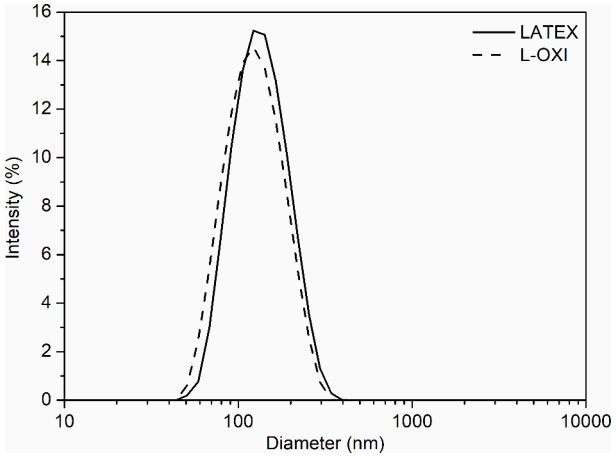

Figure 5. PSD of the poly(thioether-ester) nanoparticles before (Latex) and after oxidation (L-OXI).

polymer chains and water and can potentially be harnessed in the design of biomaterials for *in vivo* applications. The postpolymerization oxidation of thioether-containing polymers into their corresponding sulfoxide or sulfone derivatives increases the polarity of this polymer.[47]

The results of the effect of pH on the stability of the latexes are presented in Tables S1 and S2 in the Supporting Information (Section 4.0). The nonoxidized latex sample exhibited drastic colloidal instability under extreme pH conditions. At pH 3, the mean diameter increased from approximately 201 nm (t = 0) to 2116 nm (t = 24 h), with a PdI of 1.0, indicating intense particle aggregation. At pH 11, the diameter increased from 701 to 1458 nm after 24 h, confirming severe destabilization. The ζ-potential at pH 3 dropped from −24.1 mV to −12.0 mV, consistent with loss of electrostatic stabilization.

The oxidized L-OXI sample maintained excellent colloidal stability across the entire pH range evaluated (3 to 11). After 24 h, the diameters remained between 169−208 nm, with PdI values below 0.36 and sufficiently negative zeta potential values

Table 2. Intensity Mean Diameter (DP) and Polydispersity Index (PdI) of the Nanoparticles and Static Water Contact Angle Measurements of the Poly(thioether-ester) before (Latex) and after Oxidation (L-OXI and S-OXI)[a]

Sample	Average Contact Angle (θ)	Interpretation	Image	DP (nm)	PdI
Latex	104.3° ± 7.0	Hydrophobic		133.7 ± 0.2	0.117 ± 0.005
L-OXI	77.5° ± 3.2	Hydrophilic		125.6 ± 0.5	0.116 ± 0.014
S-OXI	80.4° ± 2.6	Hydrophilic		-	-

[a]± Mean SD of n = 3 determinations.

https://doi.org/10.1021/acs.iecr.6c00305
Ind. Eng. Chem. Res. XXXX, XXX, XXX−XXX

(ranging from −23 mV to −62 mV). Even at pH 3, L-OXI showed only a modest increase from 205 to 208 nm, with zeta potential maintained at approximately −23 mV.

DLS results are in fair agreement with the TEM images since the particle sizes are in the same range. The latex nanoparticles presented spherical morphology in agreement with literature reports.[48] Furthermore, TEM images of the oxidized latex (L-OXI), shown in Figure 6, reveal that the spherical morphology is

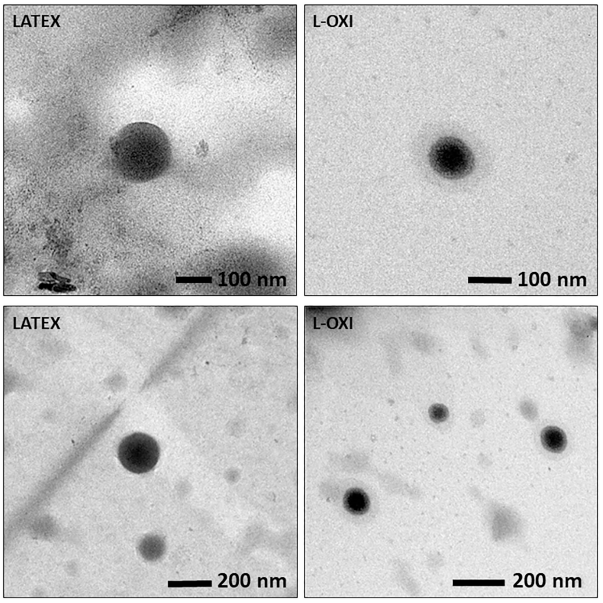

Figure 6. TEM images of the poly(thioether-ester) nanoparticles before (**Latex**) and after oxidation (**L-OXI**).

preserved after oxidation and the nanoparticles remain unchanged. To preserve the PTEe particles, TEM imaging was performed at the lowest possible beam current as they degrade under intense electron exposure. This resulted in lower resolution TEM images.

The number and weight-average molecular weights (Mn and Mw) of the poly(thioether-ester) nanoparticles (Latex) produced by miniemulsion thiol−ene polymerization using 1 wt % AIBN as the initiator were 16.8×10^3 g mol^{-1} and 51.8×10^3 g mol^{-1}, respectively.

The nonoxidized poly(thioether-ester) Latex sample showed negligible insoluble content (<4%), indicating complete solubility in THF. In contrast, both oxidized samples exhibited high insolubility in THF at 70 °C, with L-OXI presenting 83 ± 2% and S-OXI presenting 96 ± 1% insoluble polymer contents. Van Den Berg et al.[37] similarly reported that an oxidized poly(thioether) was no longer soluble in THF but could be solubilized in chloroform and aromatic solvents such as toluene and xylene at temperatures above 65 °C. In the present work, however, the oxidized samples (L-OXI and S-OXI) were insoluble in all solvents tested, including DMSO, toluene, xylene, THF, and chloroform, even under constant stirring at 70 °C for 24 h. Although both L-OXI and S-OXI dissolved in *N*-Methyl-2-pyrrolidone (NMP) at 60 °C, the solutions turned turbid upon cooling to room temperature, indicating that solubility of oxidized polymers in NMP is limited to elevated temperatures and that the polymers precipitate upon cooling, suggesting a temperature-dependent solubility behavior. The ability to dissolve in NMP, albeit only at high temperature, confirms that the oxidized polymers are not cross-linked. Nevertheless, GPC characterization of these samples was not feasible, as the available equipment was incompatible with NMP at 60 °C as eluent.

To evaluate the polymeric structure's susceptibility to biological degradation, enzymatic degradation assays were performed on Latex and L-OXI samples. CalB is known to hydrolyze ester bonds in aliphatic polyesters, including poly(thioether-ester),[20] in aqueous media and has recently been explored as a strategy to control polymer lifetime.[49,50] The thermogravimetric analysis (TGA) profiles of the polymers following 24 h of enzymatic degradation are presented in Figure 7.

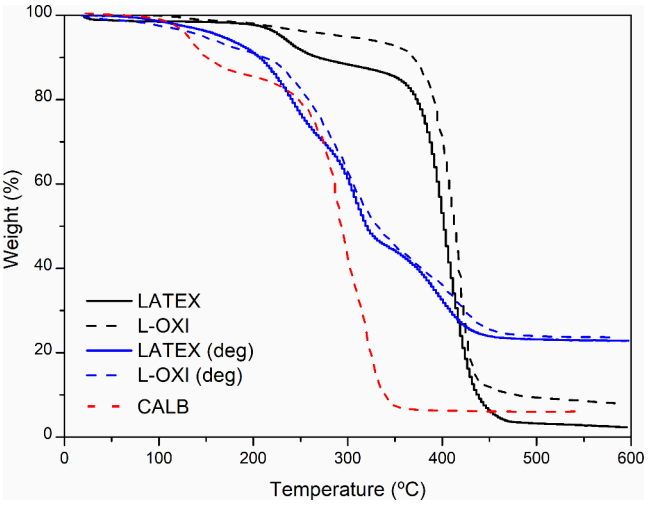

Figure 7. TGA of Latex and L-OXI original samples (in black) after and in the presence of CalB for 24 h (in blue) and CalB (in red).

TGA curves of the nonoxidized (Latex) and oxidized (L-OXI) nanoparticles exhibited a significant change in their thermal degradation profile when compared to the original polymers. The results indicate that, at 250 °C, samples degraded by CalB exhibited a greater mass loss than the untreated ones, supporting the conclusion that thermal degradation initiates at a lower temperature. The high residue (up to 20%) at 600 °C in the degraded Latex and L-OXI samples is likely attributed to residual, nonvolatile inorganic salts from the Phosphate-Buffered Saline (PBS) solution. Given the small polymer mass used relative to the surrounding PBS medium in the degradation assay, the resulting sample submitted for analysis contains a substantial concentration of these salts (e.g., phosphates, NaCl).

CalB enzyme itself has a residual mass of 5.7% at 600 °C. This residue is attributed to noncombustible inorganic components naturally present in the commercial enzyme, which typically contains stabilizers and salts from the fermentation and formulation process.[51] By operating under enzyme-excess conditions, any differences in degradation behavior between the nonoxidized (Latex) and oxidized (L-OXI) samples could be directly attributed to structural and chemical modifications of the polymer backbone (i.e., the presence of sulfoxide and sulfone groups) rather than to limitations in enzyme concentration.

The enzymatic activity of the CalB preparation (Lipozyme CalB L) was determined to be 9.3 U/g under the assay conditions (esterification of lauric acid and propanol at 60 °C, 60 min). The evolution of the particle size distributions during the enzymatic degradation essays of the original and of oxidized poly(thioether-ester) nanoparticles is presented in Figure 8.

https://doi.org/10.1021/acs.iecr.6c00305
Ind. Eng. Chem. Res. XXXX, XXX, XXX−XXX

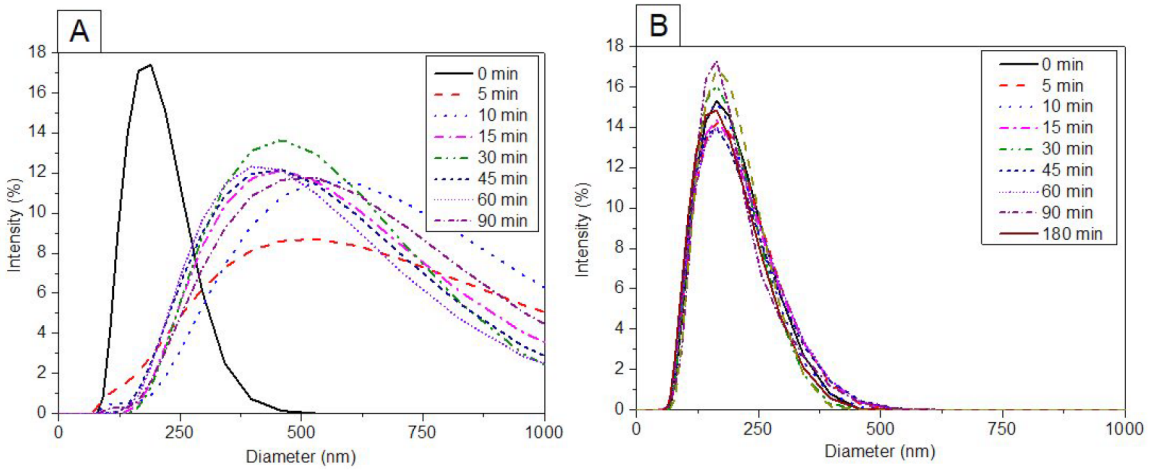

Figure 8. Evolution of the particle size distribution during the degradation of Latex and L-OXI in the presence of 1:1 CalB related to polymer in PBS. A) Latex nanoparticles; B) L-OXI nanoparticles.

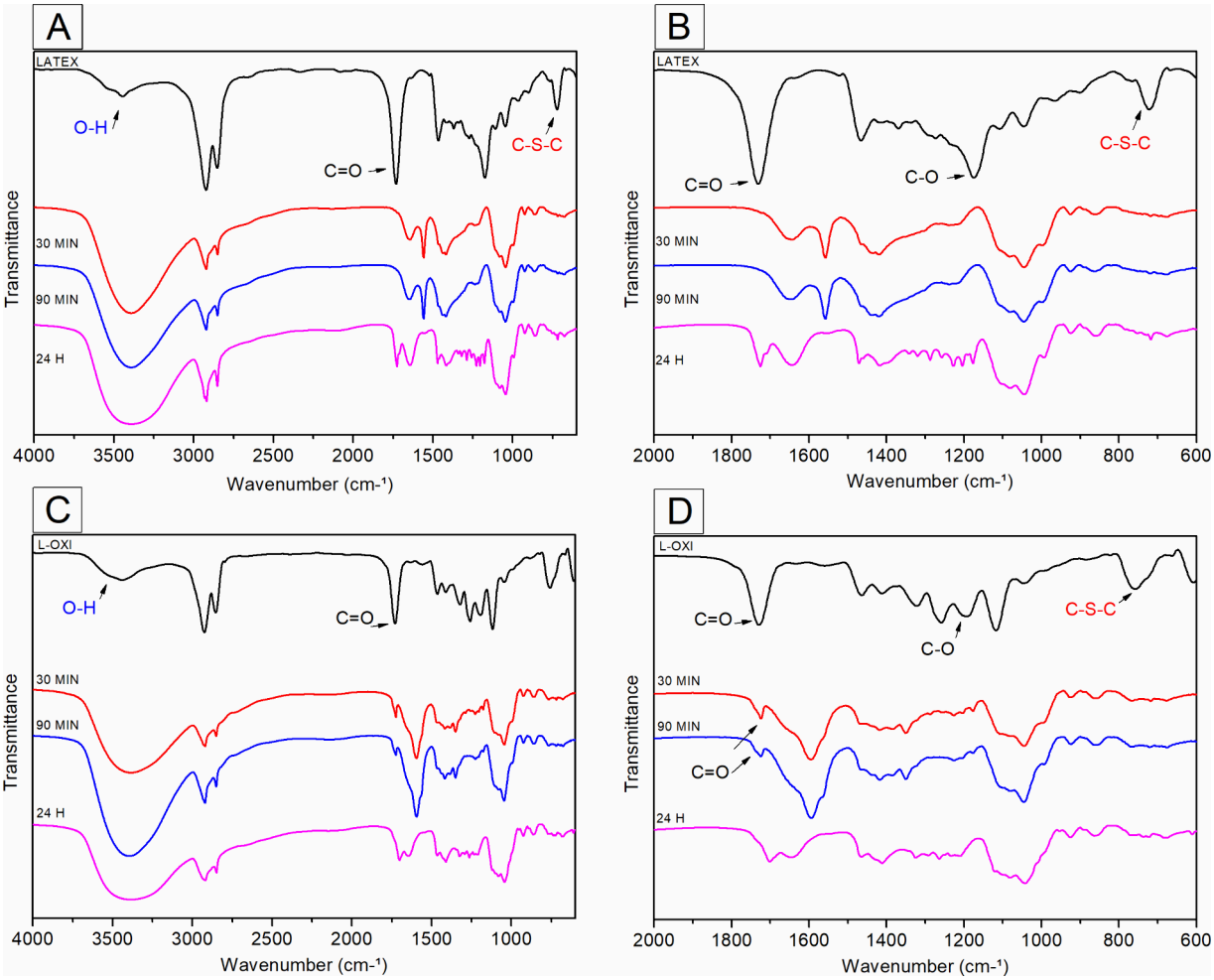

Figure 9. FTIR spectra of the Latex and L-OXI. A) Degradation with CalB 1:1 related to the polymer mass for Latex nanoparticles, after 30 min, 90 min, and 24 h. B) Enlarged View from 2000 to 600 cm^{-1} for Latex nanoparticles. C) Degradation with CalB 1:1 related to the polymer mass for the oxidized L-OXI version, after 30 min, 90 min, and 24 h. D) Enlarged View from 2000 to 600 cm^{-1} for L-OXI nanoparticles.

The mean particle size of the latex nanoparticles increases during the first 5 min in the presence of the enzyme CalB. This increase is attributed to the swelling and/or aggregation of the nanoparticles. The degradation kinetics are accelerated due to the more open conformation of the polymer chain, which facilitates enzyme access for attack. However, this effect is not observed in the L-OXI samples, where the nanoparticle size remains constant during the first 3 h. The higher stability toward degradation of the oxidized nanoparticles compared to that of the latex nanoparticles may be attributed to the increased rigidity

https://doi.org/10.1021/acs.iecr.6c00305
Ind. Eng. Chem. Res. XXXX, XXX, XXX−XXX

and insolubility of the polymer matrix. Such changes are caused by the formation of sulfoxide and sulfone groups, which in turn reduce the accessibility of the CalB enzyme to the cleavage sites. Nevertheless, it is important to mention that it was not possible to measure the particle size (DLS) of any sample, nonoxidized or oxidized, after a 24-h exposure to the enzyme CalB. On the other hand, it was verified that it was still not possible to solubilize the L-OXI nanoparticles in organic solvents (chloroform, THF, and DMSO), even after 24 h of degradation with CalB.

Some ester bonds are intrinsically more susceptible to hydrolysis due to factors such as higher electrophilicity or accessibility to water.[50] In this study, CalB hydrolyzes the available ester bonds, and an explanation for the observed size increase in the latex nanoparticles is related to the formation of acidic degradation products. These products may promote water uptake into the polymer matrix, inducing swelling.

The degradation rate of polyesters depends not only on the hydrophilicity of the polymer structure but also on its degree of crystallinity.[41,52] Figure 9 illustrates the FTIR analysis of enzymatic degradation in the presence of a 1:1 CalB-to-polymer ratio for both the Latex and L-OXI nanoparticles. After enzymatic degradation, the polymer samples became highly viscous for both samples and could not be purified by centrifugation or washing cycles. Consequently, FTIR analysis was performed directly on the degradation medium, which contained the remaining polymer, enzyme, salts and degradation products. FTIR spectra of the mixtures of the Latex and L-OXI with deactivated CalB (*see* Figure S6 in the Supporting Information) demonstrate that the bands of the enzyme overlap with the spectral regions associated with sulfoxide and sulfone groups[53], complicating the assignment of these functionalities. The decrease in C−S−C stretching band intensity (~720 cm^{-1}) observed upon mixing with deactivated CalB suggests that enzyme loading influences the FTIR signal in this region. Therefore, this spectral change cannot be used as evidence for enzymatic cleavage of thioether bonds, consistent with the reported inability of CalB to cleave C−S−C linkages.[20]

Degradation of the PTEe nanoparticles in Latex form proceeds primarily via ester bond hydrolysis, as CalB selectively catalyzes the hydrolysis of ester linkages (−C(=O)−O−) along the polymer backbone. This is evidenced by the characteristic carbonyl stretching band at 1730^{-1}, whose intensity decreased markedly after 30 min of enzymatic exposure, confirming progressive ester bond cleavage. Taken together, the full spectral data set provides a coherent picture of the degradation evolution in these polymers.

4. CONCLUSION

Poly(thioether-ester) nanoparticles produced via thiol−ene miniemulsion polymerization were successfully modified by postpolymerization oxidation with a hydrogen peroxide solution (H_2O_2), introducing sulfoxide and sulfone groups that fundamentally altered the material's properties and degradation behavior. These structural changes were confirmed by FTIR and Raman spectroscopies.

Two oxidation routes were successfully developed and characterized. Direct latex oxidation (L-OXI) is a single-step aqueous-based process that preserves nanoparticle size, morphology, and colloidal stability while avoiding organic solvents, making it attractive for applications where aqueous dispersions are desirable. Oxidation in solution (S-OXI) is a multistep process using organic solvents that yields higher purity and superior thermal stability, making it suitable for high-temperature processing techniques such as injection molding or extrusion. The choice of the method depends on the target application, with L-OXI recommended when colloidal integrity and process simplicity are priorities and S-OXI preferred when maximum purity and thermal stability are required.

While regarding colloidal stability, whereas nonoxidized nanoparticles aggregated severely at pH 3 and pH 11, L-OXI nanoparticles maintained excellent colloidal stability across the full pH range tested (3−11), with hydrodynamic average diameters of 169−208 nm and stable zeta potential values after 24 h. These results support their potential for drug delivery in physiologically relevant pH environments.

Oxidation process significantly altered the material's properties, and a profound shift in surface character was observed, with the material transitioning from a hydrophobic state, evidenced by a water contact angle of approximately 104°, to a more hydrophilic one, with a contact angle in the range of 77−80°.

Enzymatic degradation studies demonstrated that oxidation significantly enhances nanoparticle stability and imparts a sustained degradation profile relative to nonoxidized counterparts. While the ester bonds in the latex nanoparticles were rapidly hydrolyzed by CalB within minutes, L-OXI nanoparticles demonstrated remarkable resistance to enzymatic degradation, with ester bonds remaining largely intact even after 90 min of exposure. This resistance is attributed to the introduction of polar sulfoxide and sulfone groups, which increase polymer rigidity and insolubility, thereby creating a conformational barrier that physically hinders enzyme access to the hydrolyzable ester bonds. Taken together, these properties, tunable degradability through the combination of ester and thioether functional groups, enhanced colloidal stability, and controlled enzymatic resistance, position these nanoparticles as promising candidates for sustained drug release applications.

■ ASSOCIATED CONTENT

Supporting Information

(file type, i.e., PDF). The Supporting Information is available free of charge at https://pubs.acs.org/doi/10.1021/acs.iecr.6c00305.

Molecular structures obtained in each of the sample preparation steps; DTG from Latex, L-OXI, and S-OXI samples; ^{1}H NMR spectra of the monomer and the polymer; effect of pH on the stability of Latex and L-OXI; FTIR of mixtures of Latex, L-OXI and deactivated CalB (PDF)

■ AUTHOR INFORMATION

Corresponding Author

Pedro H. H. de Araújo − *Department of Chemical Engineering and Food Engineering, Universidade Federal de Santa Catarina - EQA/UFSC - C.P. 476, 88040-900 Florianópolis, Santa Catarina, Brazil;* orcid.org/0000-0001-5905-0158; Email: pedro.h.araujo@ufsc.br

Authors

Kainan A. Weege − *Department of Chemical Engineering and Food Engineering, Universidade Federal de Santa Catarina - EQA/UFSC - C.P. 476, 88040-900 Florianópolis, Santa Catarina, Brazil*

Priscilla B. Cardoso − *Department of Chemical Engineering and Food Engineering, Universidade Federal de Santa*

https://doi.org/10.1021/acs.iecr.6c00305
Ind. Eng. Chem. Res. XXXX, XXX, XXX−XXX

Catarina - EQA/UFSC - C.P. 476, 88040-900 Florianópolis, Santa Catarina, Brazil

Tamara Agner − *Department of Chemical Engineering and Food Engineering, Universidade Federal de Santa Catarina - EQA/UFSC - C.P. 476, 88040-900 Florianópolis, Santa Catarina, Brazil;* orcid.org/0000-0003-2862-9487

Claudia Sayer − *Department of Chemical Engineering and Food Engineering, Universidade Federal de Santa Catarina - EQA/UFSC - C.P. 476, 88040-900 Florianópolis, Santa Catarina, Brazil;* orcid.org/0000-0003-1044-2905

Ana P. S. Immich − *Department of Chemical Engineering and Food Engineering, Universidade Federal de Santa Catarina - EQA/UFSC - C.P. 476, 88040-900 Florianópolis, Santa Catarina, Brazil;* orcid.org/0000-0001-6927-8041

Michael A. R. Meier − *Karlsruhe Institute of Technology (KIT), Institute of Organic Chemistry (IOC) and Institute of Biological and Chemical Systems − Functional Molecular Systems (IBCS-FMS), 76131 Karlsruhe, Germany;* orcid.org/0000-0002-4448-5279

Complete contact information is available at: https://pubs.acs.org/10.1021/acs.iecr.6c00305

Author Contributions

The manuscript was written through the contributions of all authors. All authors have approved the final version of the manuscript.

Funding

Coordenação de Aperfeiçoamento de Pessoal de Nível Superior (CAPES), Conselho Nacional de Desenvolvimento Cientifico e Tecnológico (CNPq) and INCT Circularity in Polymer Materials (grant No. 406925/2022−4). The Article Processing Charge for the publication of this research was funded by the Coordenacao de Aperfeicoamento de Pessoal de Nivel Superior (CAPES), Brazil (ROR identifier: 00x0ma614).

Notes

The authors declare no competing financial interest.

■ ACKNOWLEDGMENTS

The authors thank Coordenação de Aperfeiçoamento de Pessoal de Nível Superior (CAPES) and Conselho Nacional de Desenvolvimento Científico e Tecnológico (CNPq) for financial support and the Laboratório Central de Microscopia Eletrônica (LCME) at Universidade Federal de Santa Catarina (UFSC) for the TEM analyses.

■ ABBREVIATIONS

PTEe, Poly(thioether-ester); L-OXI, Latex oxidized; S-OXI, Solution oxidized; SDS, Sodium dodecyl sulfate; AIBN, 2,2′-Azobis(2-methylpropionitrile); H_2O_2, Hydrogen peroxide; TGA, Thermogravimetric analysis; DSC, Differential scanning calorimetry; DLS, Dynamic light scattering; TEM, Transmission electron microscopy; ATR-FTIR, Attenuated Total Reflectance-Fourier Transform Infrared; PDI, Polydispersity index

■ REFERENCES

(1) Meier, M. A. R. Renewable Resources for Polymer Chemistry: A Sustainable Alternative? *Macromol. Rapid Commun.* **2011**, *32* (17), 1297−1298.

(2) Montero de Espinosa, L.; Meier, M. A. R. Plant Oils: The Perfect Renewable Resource for Polymer Science?! *Eur. Polym. J.* **2011**, *47* (5), 837−852.

(3) Rajput, C. V.; Sastry, N. V.; Chikhaliya, N. P. Vegetable Oils Based Precursors: Modifications and Scope for Futuristic Bio-Based Polymeric Materials. *J. Polym. Res.* **2023**, *30* (4), 159.

(4) Jha, S.; Akula, B.; Enyioma, H.; Novak, M.; Amin, V.; Liang, H. Biodegradable Biobased Polymers: A Review of the State of the Art, Challenges, and Future Directions. *Polymers* **2024**, *16* (16), 2262.

(5) Turunc, O.; Meier, M. A. R. The Thiol-ene (Click) Reaction for the Synthesis of Plant Oil Derived Polymers. *Eur. J. Lipid Sci. Technol.* **2013**, *115*, 41−54.

(6) Luleburgaz, S.; Cakmakci, E.; Durmaz, H.; Tunca, U. Sustainable Polymers from Renewable Resources through Click and Multicomponent Reactions. *Eur. Polym. J.* **2024**, *209*, 112897.

(7) Molina-Gutiérrez, S.; Ladmiral, V.; Bongiovanni, R.; Caillol, S.; Lacroix-Desmazes, P. Radical Polymerization of Biobased Monomers in Aqueous Dispersed Media. *Green Chem.* **2019**, *21* (1), 36−53.

(8) Durham, O. Z.; Shipp, D. A. Polymer Colloids from Step-Growth Thiol-X Polymerizations. *Polym. Rev.* **2021**, *61* (1), 54−79.

(9) Herzberger, J.; Fischer, K.; Leibig, D.; Bros, M.; Thiermann, R.; Frey, H. Oxidation-Responsive and "Clickable" Poly(Ethylene Glycol) via Copolymerization of 2-(Methylthio)Ethyl Glycidyl Ether. *J. Am. Chem. Soc.* **2016**, *138* (29), 9212−9223.

(10) Işık, D.; Anand Joshi, A.; Guo, X.; Rancan, F.; Klossek, A.; Vogt, A.; Rühl, E.; Hedtrich, S.; Klinger, D. Sulfoxide-Functionalized Nanogels Inspired by the Skin Penetration Properties of DMSO. *Biomater. Sci.* **2021**, *9* (3), 712−725.

(11) Podgórski, M.; Wang, C.; Yuan, Y.; Konetski, D.; Smalyukh, I.; Bowman, C. N. Pristine Polysulfone Networks as a Class of Polysulfide-Derived High-Performance Functional Materials. *Chem. Mater.* **2016**, *28* (14), 5102−5109.

(12) Tan, J.; Li, C.; Bruycker, K. D.; Zhang, G.; Gu, J.; Zhang, Q. Recyclable Cross-Linked Hydroxythioether Particles with Tunable Structures via Robust and Efficient Thiol-Epoxy Dispersion Polymerizations. *RSC Adv.* **2017**, *7* (82), 51763−51772.

(13) Sarapas, J. M.; Tew, G. M. Thiol-Ene Step-Growth as a Versatile Route to Functional Polymers. *Angew. Chem.* **2016**, *128*, 16092−16095.

(14) Hoyle, C. E.; Lee, T. Y.; Roper, T. Thiol-Enes: Chemistry of the Past with Promise for the Future. *J. Polym. Sci. Part Polym. Chem.* **2004**, *42* (21), 5301−5338.

(15) Hoyle, C. E.; Bowman, C. N. Thiol-Ene Click Chemistry. *Angew. Chem., Int. Ed.* **2010**, *49* (9), 1540−1573.

(16) Asua, J. M. Miniemulsion Polymerization. *Prog. Polym. Sci.* **2002**, *27* (7), 1283−1346.

(17) Landfester, K. Miniemulsion Polymerization and the Structure of Polymer and Hybrid Nanoparticles. *Angew. Chem., Int. Ed.* **2009**, *48* (25), 4488−4507.

(18) Aguirre, M.; Ballard, N.; Gonzalez, E.; Hamzehlou, S.; Sardon, H.; Calderon, M.; Paulis, M.; Tomovska, R.; Dupin, D.; Bean, R. H.; Long, T. E.; Leiza, J. R.; Asua, J. M. Polymer Colloids: Current Challenges, Emerging Applications, and New Developments. *Macromolecules* **2023**, *56* (7), 2579−2607.

(19) Feuser, P. E.; Matos dos Santos, P. C.; Cordeiro, A. P.; Stefanes, N. M.; Walter, L. O.; Maioral, M. F.; Santos-Silva, M. C.; Hermes de Araújo, P. H.; Sayer, C. Antineoplastic Activity of Free 4-Nitrochalcone and Encapsulated in Poly(Thioether-Ester) Nanoparticles Obtained by Thiol-Ene Polymerization in Two Human Leukemia Cell Lines (Jurkat and K562). *J. Drug Deliv Sci. Tech* **2022**, *67*, 102924.

(20) Hoelscher, F.; Cardoso, P. B.; Candiotto, G.; Guindani, C.; Feuser, P.; Araújo, P. H. H.; Sayer, C. In Vitro Degradation and Cytotoxicity Response of Biobased Nanoparticles Prepared by Thiol-Ene Polymerization in Miniemulsion. *J. Polym. Environ.* **2021**, *29* (11), 3668−3678.

(21) Resetco, C.; Hendriks, B.; Badi, N.; Du Prez, F. Thiol-Ene Chemistry for Polymer Coatings and Surface Modification - Building in Sustainability and Performance. *Mater. Horiz.* **2017**, *4* (6), 1041−1053.

(22) Sarapas, J. M.; N. Tew, G. Poly(Ether-Thioethers) by Thiol-Ene Click and Their Oxidized Analogues as Lithium Polymer Electrolytes. *Macromolecules* **2016**, *49*, 1154−1162.

(23) Hobiger, V.; Koler, A.; Kotek, J.; Krajnc, P. Emulsion Templated Poly(Thiol-Enes): Selective Oxidation Improves Mechanical Properties. *React. Funct Polym.* **2023**, *186*, 105551.
(24) Potapov, A. S.; Chernova, N. P.; Ogorodnikov, V. D.; Petrenko, T. V.; Khlebnikov, A. I. Synthesis and Oxidation of Some Azole-Containing Thioethers. *Beilstein J. Org. Chem.* **2011**, *7*, 1526−1532.
(25) Vo, C. D.; Kilcher, G.; Tirelli, N. Polymers and Sulfur: What Are Organic Polysulfides Good For? *Preparative Strategies and Biological Applications.* **2009**, *30*, 299−315.
(26) Sarapas, J. M.; Tew, G. N. Thiol-Ene Step-Growth as a Versatile Route to Functional Polymers. *Angew. Chem., Int. Ed.* **2016**, *55* (51), 15860−15863.
(27) Kupwade, R. V. A Concise Review on Synthesis of Sulfoxides and Sulfones with Special Reference to Oxidation of Sulfides. *J. Chem. Rev.* **2019**, *1* (2), 99−113.
(28) Yook, J.; Jeong, D.; Lee, J.-C. Synthesis of Citronellol-Derived Antibacterial Polymers and Effect of Thioether, Sulfoxide, Sulfone, and Ether Functional Groups on Their Bactericidal Activity. *Macromolecules* **2023**, *56* (9), 3406−3420.
(29) Infante Teixeira, L.; Landfester, K.; Thérien-Aubin, H. Selective Oxidation of Polysulfide Latexes to Produce Polysulfoxide and Polysulfone in a Waterborne Environment. *Macromolecules* **2021**, *54* (8), 3659−3667.
(30) Perell, G. T.; Staebell, R. L.; Hairani, M.; Cembran, A.; Pomerantz, W. C. K. Tuning Sulfur Oxidation States on Thioether-Bridged Peptide Macrocycles for Modulation of Protein Interactions. *Chembiochem.* **2017**, *18* (18), 1836−1844.
(31) Jasinski, F.; Rannée, A.; Schweitzer, J.; Fischer, D.; Lobry, E.; Barghorn, C. C.; Schmutz, M.; Le Nouen, D.; Criqui, A.; Chemtob, A. Thiol-Ene Linear Step-Growth Photopolymerization in Miniemulsion: Fast Rates, Redox-Responsive Particles, and Semicrystalline Films. *Macromolecules* **2016**, *49*, 1143−1153.
(32) Jereb, M. Highly Atom-Economic, Catalyst- and Solvent-Free Oxidation of Sulfides into Sulfones Using 30% Aqueous H2O2. *Green Chem.* **2012**, *14* (11), 3047−3052.
(33) Valverde, C.; Lligadas, G.; Ronda, J. C.; Galià, M.; Cádiz, V. Synthesis and Characterization of Castor Oil-Derived Oxidation-Responsive Amphiphilic Block Copolymers: Poly(Ethylene Glycol)-b-Poly(11-((2-Hydroxyethyl)Thio)Undecanoate). *Eur. Polym. J.* **2020**, *133*, 109736.
(34) Noyori, R.; Aoki, M.; Sato, K. Green Oxidation with Aqueous Hydrogen Peroxide. *Chem. Commun.* **2003**, No. 16, 1977−1986.
(35) Jeanmaire, D.; Laliturai, J.; Almalik, A.; Carampin, P.; d'Arcy, R.; Lallana, E.; Evans, R.; Winpenny, R. E. P.; Tirelli, N. Chemical Specificity in REDOX-Responsive Materials: The Diverse Effects of Different Reactive Oxygen Species (ROS) on Polysulfide Nanoparticles. *Polym. Chem.* **2014**, *5* (4), 1393−1404.
(36) Cardoso, P. B.; Machado, T. O.; Feuser, P. E.; Sayer, C.; Meier, M. A. R.; Araújo, P. H. H. Biocompatible Polymeric Nanoparticles From Castor Oil Derivatives via Thiol-Ene Miniemulsion Polymerization. *Eur. J. Lipid Sci. Technol.* **2018**, *120* (1), 1700212.
(37) Van Den Berg, O.; Dispinar, T.; Hommez, B.; Du Prez, F. E. Renewable Sulfur-Containing Thermoplastics via AB-Type Thiol-Ene Polyaddition. *Eur. Polym. J.* **2013**, *49* (4), 804−812.
(38) Oliveira, D.; Feihrmann, A. C.; Rubira, A. F.; Kunita, M. H.; Dariva, C.; Oliveira, J. V. Assessment of Two Immobilized Lipases Activity Treated in Compressed Fluids. *J. Supercrit. Fluids* **2006**, *38* (3), 373−382.
(39) Meneses, A. C. d.; Machado, T. O.; Araújo, P. H. H.; de Oliveira, D.; et al. Development Of Antioxidant Poly(Thioether-Ester) Nanoparticles. *Braz. J. Chem. Eng.* **2018**, *35* (2), 691.
(40) Fokou, P. A.; Meier, M. A. R. Studying and Suppressing Olefin Isomerization Side Reactions During ADMET Polymerizations. *Macromol. Rapid Commun.* **2010**, *31* (4), 368−373.
(41) Fulajtar, E.; Agarwal, S. From Thioether to Sulfone: Transforming Polyester Properties for Enhanced Degradation. *ACS Appl. Polym. Mater.* **2024**, *6* (17), 10768−10778.
(42) Rajawasam, C. W. H.; Dodo, O. J.; Weerasinghe, M. A. S. N.; Raji, I. O.; Wanasinghe, S. V.; Konkolewicz, D.; Watuthanthrige, N. D. A. Educational Series: Characterizing Crosslinked Polymer Networks. *Polym. Chem.* **2024**, *15*, 219.
(43) Infante Teixeira, L. I.; Landfester, K.; Thérien-Aubin, H. Selective Oxidation of Polysulfide Latexes to Produce Polysulfoxide and Polysulfone in a Waterborne Environment. *Macromolecules* **2021**, *54* (8), 3659−3667.
(44) Mattos dos Santos, P. C.; Feuser, P. E.; Cardoso, P. B.; Steiner, B. T.; Córneo, E. da S.; Scussel, R.; Viegas, A. da C.; Machado-de-Ávila, R. A.; Sayer, C.; Hermes de Araújo, P. H. Evaluation of in Vitro Cytotoxicity of Superparamagnetic Poly(Thioether-Ester) Nanoparticles on Erythrocytes, Non-Tumor (NIH3T3), Tumor (HeLa) Cells and Hyperthermia Studies. *Biomater Sci.* **2018**, *29* (16), 1935.
(45) Herzberger, J.; Fischer, K.; Leibig, D.; Bros, M.; Thiermann, R.; Frey, H. Oxidation-Responsive and "Clickable" Poly(Ethylene Glycol) via Copolymerization of 2-(Methylthio)Ethyl Glycidyl Ether. *J. Am. Chem. Soc.* **2016**, *138* (29), 9212−9223.
(46) Rajes, K.; Walker, K. A.; Hadam, S.; Zabihi, F.; Ibrahim-Bacha, J.; Germer, G.; Patoka, P.; Wassermann, B.; Rancan, F.; Rühl, E.; Vogt, A.; Haag, R. Oxidation-Sensitive Core-Multishell Nanocarriers for the Controlled Delivery of Hydrophobic Drugs. *ACS Biomater Sci. Eng.* **2021**, *7* (6), 2485−2495.
(47) Ren, T.; Chen, Q.; Zhao, C.; Zheng, Q.; Xie, H.; North, M. Introducing the Tishchenko Reaction into Sustainable Polymer Chemistry. *Green Chem.* **2020**, *22* (5), 1542−1547.
(48) Freire, N. F.; Feuser, Paulo Emílio; da Silva Abel, Jéssica; Machado-de-Ávila, Ricardo Andrez; Lopes Fialho, Rosana; Cabral Albuquerque, Elaine; Sayer, Claudia; Hermes de Araújo, P. H. Zinc Phthalocyanine Encapsulation via Thiol-Ene Miniemulsion Polymerization and in Vitro Photoxicity Studies. *Int. J. Polym. Mater. Polym. Biomater.* **2022**, *71* (5), 349−358.
(49) Mafakheri, F.; Khoee, S. Synthesis of Candida Antarctica Lipase B (CALB) Enzyme-Powered Magnetite Nanomotor Based on PCL/Chitosan Janus Nanostructure. *Sci. Rep.* **2022**, *12*, 12758.
(50) Ganesh, M.; Gross, R. A. Embedded Enzymatic Biomaterial Degradation: Flow Conditions & Relative Humidity. *Polymer* **2012**, *53* (16), 3454−3461.
(51) Llerena-Suster, C. R.; Briand, L. E.; Morcelle, S. R. Analytical Characterization and Purification of a Commercial Extract of Enzymes: A Case Study. *Colloids Surf. B Biointerfaces* **2014**, *121*, 11−20.
(52) Aarsen, C. V.; Liguori, A.; Mattsson, R.; Sipponen, M. H.; Hakkarainen, M. Designed to Degrade: Tailoring Polyesters for Circularity. *Chem. Rev.* **2024**, *124* (13), 8473−8515.
(53) Zdarta, J.; Klapiszewski, L.; Jedrzak, A.; Nowicki, M.; Moszynski, D.; Jesionowski, T. Lipase B from Candida Antarctica Immobilized on a Silica-Lignin Matrix as a Stable and Reusable Biocatalytic System. *Catalysts* **2017**, *7* (1), 14.

https://doi.org/10.1021/acs.iecr.6c00305
Ind. Eng. Chem. Res. XXXX, XXX, XXX−XXX